Modeling and Simulation of the Phase-Inversion Process During Membrane Preparation

G. R. FERNANDES, J. C. PINTO, R. NOBREGA

COPPE/Chemical Engineering Program, Federal University of Rio de Janeiro, P.O. Box 68502, Rio de Janeiro 21945-970, Brazil

Received 15 November 2000; accepted 4 April 2001

ABSTRACT: The objective of this work is to present a simple mathematical model to describe the main features of phase inversion by immersion precipitation. The model was developed for planar geometry and is used to simulate membrane synthesis. Two systems commonly used for membrane preparation were used for simulations: cellulose acetate/acetone/water and polyetherimide/*N*-methylpyrrolidone/water. The influence of nonsolvent addition to initial polymer casting solutions, solvent addition to the coagulation bath, and geometric variables, such as polymer film thickness, on the final precipitation conditions were studied through simulation and compared to available experimental data. The results are in good agreement with published results.[1–3] It is shown that polymer film composition profiles at the moment of precipitation may give important information about the structure and substructure of formed membrane. It is also shown, for both polymeric systems investigated in this work, that the dynamics of the mass transfer process seems to be much more important than the influence of the concentration on the diffusion and thermodynamic partition coefficients, as fair agreement with available experimental data was obtained even when these coefficients were assumed to be constant. © 2001 John Wiley & Sons, Inc. J Appl Polym Sci 82: 3036–3051, 2001

Key words: membranes; modeling; phase separation; membrane preparation; phase inversion; mathematical model; polymer solution

INTRODUCTION

Polymer membranes are widely used for the separation of chemical constituents and the purification of process streams in many important industrial fields. Usual applications include solid–liquid separations, removal of ethanol from aqueous solutions, and gas separations.[4] These polymer membranes are usually prepared through phase inversion, where a polymer solution (containing the polymer species and a solvent) is immersed in a coagulation bath (containing a chemical component, the nonsolvent, that is compatible with the solvent but does not dissolve the polymer species), which forces the polymer precipitation and the formation of a polymer film membrane.[3] The final membrane properties are known to depend on the precipitation conditions and variables such as the initial polymer concentration in the polymer casting solution, initial solvent concentration in the coagulation bath, relative amounts of polymer and nonsolvent in casting solutions, and so on, which may exert a major impact on the final performance of the membrane.[5] Therefore, the appropriate understanding of the phase-inversion phenomena and the development of mathematical models to describe the membrane formation may be of great value for those interested in membrane synthesis and its applications.

Correspondence to: R. Nobrega (nobrega@peq.coppe.ufrj.br).

Journal of Applied Polymer Science, Vol. 82, 3036–3051 (2001)

Few models are available in the literature to describe the phase-inversion process on planar systems.[3,5–13] Because the phase-inversion process depends on the equilibrium thermodynamics of the system, the surface properties of the interface that separates the polymer solution and the coagulation bath, and the mass transfer of the chemical species added to both solutions and because fast polymer precipitation leads to the development of huge concentration gradients in both polymer and coagulation solutions, these models present a very detailed description of the precipitation mechanism. For this reason, except in the case of molecular modeling proposed by Termonia,[9] these models depend on parameters that are difficult to obtain in the open literature (e.g., ternary diffusion coefficients and the concentration dependence of diffusion coefficients and thermodynamics parameters) and difficult to estimate *a priori* on the basis of known constitutive equations. Besides, the final model structure may become very complex, in the sense that the model is constituted by a coupled set of partial differential equations that depend on time-varying parameters that may be unbounded at certain preparation conditions, especially in the very beginning of the simulation.[3 [eqs. 50–60]] After discretization, due to the intrinsic nature of the available models and due to the preparation conditions, the Jacobian matrix is full at each discretization grid point, and the discretized system of ordinary differential equations may be very stiff. This means that very small integration steps and a very large computation time may be required for simulation of the phase-inversion model. As model solutions may be very complex and may depend on many physical parameters that almost always are unknown, they can seldom be applied to practical purposes, such as the preliminary investigation of the effects of phase-inversion operation variables on precipitation conditions, in the form presented. This is especially true during the screening stages of membrane development, when large sets of possible preparation conditions are taken into consideration and most conditions are discarded before actual experiments are carried out.

The models described previously are based on the Maxwell–Stefan equations,[4] where diffusion coefficients depend on the local states of the solution and cross-diffusion terms are not neglected. The Flory–Huggins equation[13] is used to describe the local activities of the chemical components and the thermodynamic equilibrium at the interface. The coefficients are also assumed to depend on the local states of both solutions. The model structure comprises a set of nonlinear, coupled partial differential equations with time-dependent and moving boundary conditions. The cellulose acetate (AC)/acetone/water system is generally used to validate the models because model parameters needed to simulate the phase-inversion process may be evaluated from available experimental data in this case.

The goal of this work was to develop a much simpler phase-inversion model that could be used for practical purposes for those involved with membrane preparation and that would relax some of the usual assumptions and reduce the number of parameters needed for simulations. The main objective was to provide a simple mathematical structure that could be used to simulate how concentration gradients change in each phase as certain key preparation variables, such as initial concentration, are changed. The model must describe the phase-inversion conditions and the precipitation lag time as functions of the preparation conditions. Polymer, solvent, and nonsolvent concentrations at the interface during polymer precipitation and the concentration gradients inside individual phases provide information about the structure of the membrane.[5,10,13,14] Precipitation time provides fundamental information for membrane manufacture and process design and is also useful for parameter estimation, as precipitation time may be easily obtained in the lab from standard kinetic experiments.[2]

It is shown here that a very simple mathematical model may be built to allow the simulation of phase-inversion phenomena. The model combines simple mass balance equations for the different chemical components in the different phases with a thermodynamic equilibrium constraint. Besides the thermodynamic equilibrium relationship, the model depends only on a set of constant binary coefficients (diffusion coefficients) that may be obtained in the open literature[15] or may be computed with the help of known constitutive equations.[16] Additionally, model equations are coupled through simple linear algebraic constraints, which means that standard integration procedures such as DASSL[17] are able to integrate the model very efficiently. It is shown here that such a model can be used very successfully to describe the phase-inversion phenomena during membrane preparation and can be used for practical purposes and the preliminary investigation of

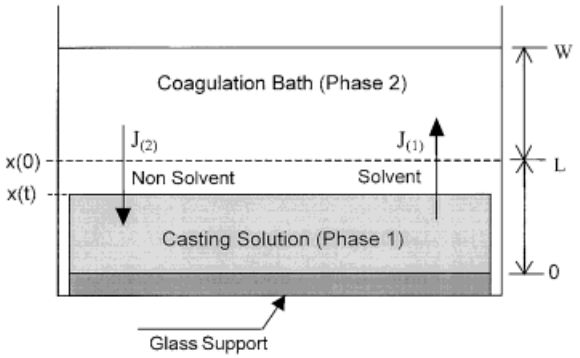

Figure 1 Schematic representation of the phase-inversion process.

membrane preparation conditions, despite the much less rigorous derivation of model equations.

MATHEMATICAL MODEL

The phase-inversion process is schematically represented in Figure 1. A thin film of a certain polymer solution (Phase 1, which contains the polymer constituent, the solvent, and a certain amount of the nonsolvent) is initially casted onto a glass support. This step is usually called the casting step. This solution is then immersed into an appropriate coagulation bath (Phase 2, which contains the nonsolvent and a certain amount of the solvent). This step is normally called the quenching step. An intermediate step, called the evaporation step, where the initial polymer solution is exposed to a controlled gas atmosphere to allow the manipulation of the initial gradients in the polymer solution, is sometimes performed before the immersion into the coagulation bath. This step is not covered in this work, but the model presented can be easily extended to include this step. The result of the phase-inversion process is the production of an asymmetric polymer film with one thin and relative dense skin and a porous sublayer.

The formed membrane must show high permeability and high selectivity. These properties may be correlated to the membrane morphology so that polymer concentrations during precipitation may give clues in regard to the final properties of the membrane.[5] During the quenching step, a significant mass exchange of solvent and nonsolvent occurs through the casting solution/bath coagulation interface. The mass transfer between the two phases leads to unstable thermodynamic conditions, and the polymer constituent eventually precipitates. Then, the casting solution gives birth to two distinct phases: a polymer-rich phase and a diluted polymer phase. The polymer phase leads to the membrane formation. If the precipitation occurs with high polymer concentrations, the membrane skin tends to be dense and very selective; otherwise, the membrane skin tends to be porous and to present low selectivity. If polymer concentration gradients are very large during precipitation, the skin and the sublayer tend to present very different properties.

Prediction of membrane morphology through simulation, based on knowledge of the initial states of both casting solution and coagulation bath, is a highly desirable objective. Although this objective is far from realistic, modeling of mass transfer phenomena during the quenching step can provide important information about the structure and substructure of the formed membrane, as discussed before. With this objective, a mass transfer model is presented later. The model is based on very simple assumptions, which include constant physical parameters, additivity of volumes, thermodynamic equilibrium at the interface (described through constant partition coefficients), absence of polymer in the coagulation bath, and the existence of one-dimensional concentration gradients. Cross-diffusion terms are neglected and the well-known Fick equations[13] are used to describe mass transfer within each phase. Despite the simplifying assumptions, the model considers that the casting solution/coagulation bath interface moves during the process.

According to the model assumptions, the mass transfer of component i within the phase j can then be written as

$$\frac{\partial C_{(i,j)}}{\partial t} = D_{(i,j)} \cdot \frac{\partial^2 C_{(i,j)}}{\partial x^2}, \begin{cases} i = 1, 2, & \text{for } j = 1 \\ i = 1, & \text{for } j = 2 \end{cases} \tag{1}$$

where $C_{(i,j)}$ is the molar concentration of component i in phase j (kg/m^3), $D_{(i,j)}$ is the diffusion coefficient of component i in phase j (m^2/s), and x is the mass transfer direction (m). This is subject to the following boundary conditions:

$$\left.\frac{\partial C_{(i,1)}}{\partial x}\right|_{x=0} = 0, \quad i = 1, 2, \text{ for } j = 1 \tag{2}$$

$$\left.\frac{\partial C_{(i,2)}}{\partial x}\right|_{x=W} = 0, \quad i = 1, \text{ for } j = 2 \tag{3}$$

Table I Typical Values for the Diffusion Coefficient[a]

Component	Phase	Diffusion Coefficient (m^2/s)
Solvent	Polymer solution	1×10^{-11}
Nonsolvent	Polymer solution	1×10^{-11}
Solvent	Coagulation bath	1×10^{-9}
Nonsolvent	Coagulation bath	1×10^{-9}

[a] Reuvers and Smolders.[2]

$$C_{(i,1)}|_L = k_{(i)} \cdot C_{(i,2)}|_L, \quad i = 1, 2 \tag{4}$$

$$D_{(i,1)} \cdot \left.\frac{\partial C_{(i,1)}}{\partial x}\right|_{x=L} = D_{(i,2)} \cdot \left.\frac{\partial C_{(i,2)}}{\partial x}\right|_{x=L}, \quad i = 1, 2 \tag{5}$$

where L is the casting solution thickness at time t (m), $k_{(i)}$ is the partition coefficient of component i, and W is the external limit of the coagulation bath.

Equations (2) and (3) mean that there is no mass exchange through the borders of the system. Equation (4) describes the local thermodynamic equilibrium at the interface, and Equation (5) describes the mass transfer continuity at both sides of the interface.

Assuming that the initial solutions are homogeneous, it is possible to write

$$C_{(i,j)}|_{t=0} = C_{0(i,j)}, \; i, \quad j = 1, 2 \tag{6}$$

The global mass balance equation may be written as

$$\sum_{i=1}^{NC} \phi_{(i,j)} = 1 \tag{7}$$

where NC is the number of chemical species and $\phi_{(i,j)}$ is the volume fraction of component i in the phase j, defined as

$$\phi_{(i,j)} = \frac{C_{(i,j)} \cdot Pm_{(i)}}{\rho_{(i)}} \tag{8}$$

where $Pm_{(i)}$ is the molecular weight of component i (kg/kmol) and $\rho_{(i)}$ is the density of the pure component i, so that the polymer composition in the casting solution is

$$C^*_{(3,1)} = \rho_{(3,1)} \cdot \left[1 - \left(\frac{Pm_{(1,1)}}{\rho_{(1,1)}} \cdot C_{(1,1)}\right) - \left(\frac{Pm_{(2,1)}}{\rho_{(2,1)}} \cdot C_{(2,1)}\right)\right] \tag{9}$$

where $C^*_{(i,j)}$ is the mass concentration of component i in phase j (mol/m^3) and $\rho_{(i,j)}$ is the density of component i in phase j, whereas the nonsolvent concentration in the coagulation bath is

$$C_{(2,2)} = \left(\frac{\rho_{(2,2)}}{Pm_{(2,2)}}\right) \cdot \left[1 - \left(\frac{Pm_{(1,2)}}{\rho_{(1,2)}} \cdot C_{(1,2)}\right)\right] \tag{10}$$

Finally, the interface displacement velocity can be derived from the global mass balance equation of the polymer species. The polymer mass is assumed to be constant and completely contained by the casting solution. Thus

$$M_{(3,1)} = A \cdot \int_0^L C_{(3,1)} \cdot dx \tag{11}$$

where $M_{(3,1)}$ is the total polymer mass in polymer solution (kg) and A is the flow transversal area (m^2). If eq. (11) is derived in respect to time and made equal to zero, then

$$\frac{dL}{dt} = -\frac{1}{C_{(3,1)}|_L} \cdot \int_0^L \frac{dC_{(3,1)}}{dt} \cdot dx \tag{12}$$

which is the convective interface displacement velocity.

Equations (1–12) constitute the mathematical model used here to simulate the phase-inversion phenomena. For the model to be solved, it is necessary to know the molecular weights, densities, partition coefficients, and diffusion coefficients for all the chemical species involved. The first two

Table II Physical Properties for AC/Acetone/Water System[a]

Component	Density (kg/m^3)	Molecular Weight (kg/kmol)
AC	1.428	27,000
Acetone	757	58
Water	997	18

[a] Reuvers and Smolders.[2]

Table III Physical Properties for PEI/NMP/Water System[a]

Component	Density (kg/m^3)	Molecular Weight (kg/kmol)
PEI	1370	22,400
NMP	1027	96.13
Water	997	18.0

[a] Furtado.[18]

sets of parameters are assumed to be known. The partition coefficients may be estimated from simple static phase-separation experiments.[18] Although we are aware that partition coefficients may depend on the local states of the system, changes of orders of magnitude are not expected, so rough estimates of these parameters can be obtained very easily, either experimentally or through simulation. Diffusion coefficients may be estimated from dynamic experiments (which is time consuming and difficult to do in the lab) or may be guessed from published data with accuracy within an order of magnitude.

The model parameters used in these simulations were obtained from published material. Diffusion coefficients were taken from Reuvers[2] and are shown in Table I. Solvent and nonsolvent partition coefficients are typical values presented by Reuvers and Smolders[2] and Furtado.[18] The typical values for partition coefficients of solvent and nonsolvent are 1.0 and 0.5, respectively. Additional physical properties were also presented by Reuvers and Smolders[2] and Furtado.[18] All parameters needed for simulation are shown in Tables I–III.

A central finite difference discretization strategy was used to provide numerical solutions of the mathematical model. This procedure transforms the model equations into a set of algebraic differential equations, which may be solved with standard numerical codes, such as DASSL.[17] To account for the moving boundary, an adaptative discretization grid scheme was used. According to this scheme, the last discretization point of each phase was placed at the interface, and its axial coordinate was allowed to vary with the interface position. As soon as the interface position crossed one of the other static discretization points, the integration was halted, the grid was updated, and the numerical procedure was reinitialized. The adaptative strategy is illustrated in Figure 2.

As the numerical integration proceeded, polymer, solvent, and nonsolvent concentrations for all discretization elements inside the casting and coagulation solutions were computed. The dynamic trajectory of the grid points and especially of the interface could then be followed graphically or numerically in a thermodynamic equilibrium chart. The equilibrium charts (the binodal curve of the system) were taken from Reuvers and Smolders[2] for the AC/acetone/water system and from Furtado[18] for the polyetherimide (PEI)/*N*-methylpyrrolidone (NMP)/water system as presented in Figure 3. As soon as the dynamic trajectory crossed the system binodal curve, it was assumed that precipitation occurred. Figure 4 illustrates the procedure.

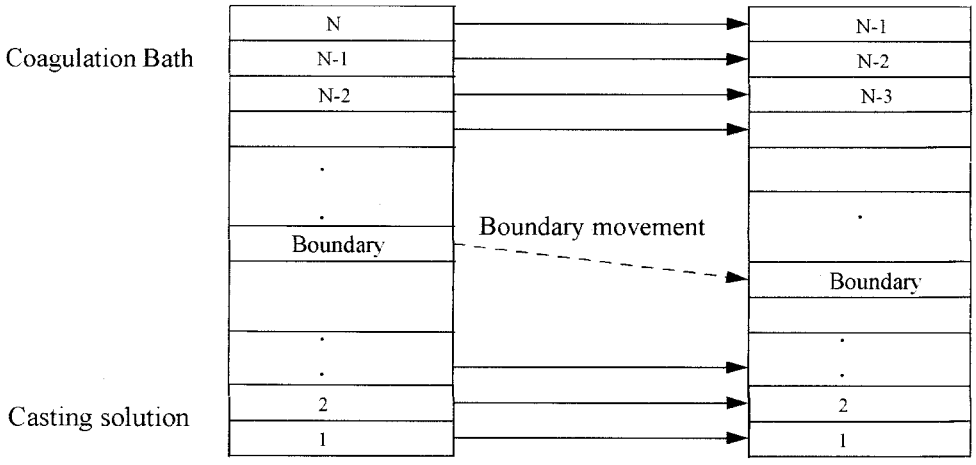

Figure 2 Numerical representation of the boundary movement.

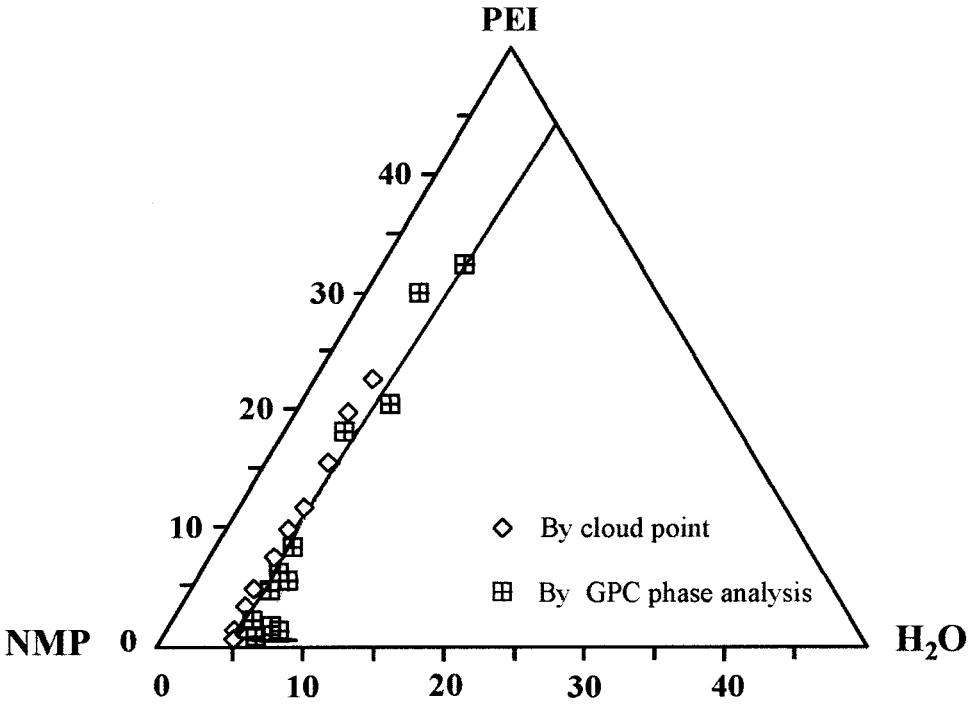

Figure 3 Phase diagram for the PEI/NMP/water system. Temperature = 25°C (from Furtado,[18] chapter 4, p 89, unpublished results).

In many polymeric systems used to prepare membranes by immersion precipitation, we can suppose, mainly on the basis of the membrane morphology, that the spinodal phase separation was present during the process. Nevertheless, in a general way, both situations (either binodal or spinodal phase separation) could occur, depending on the polymeric systems and immersion precipitation conditions. In this work, the binodal precipitation was used as the phase-separation

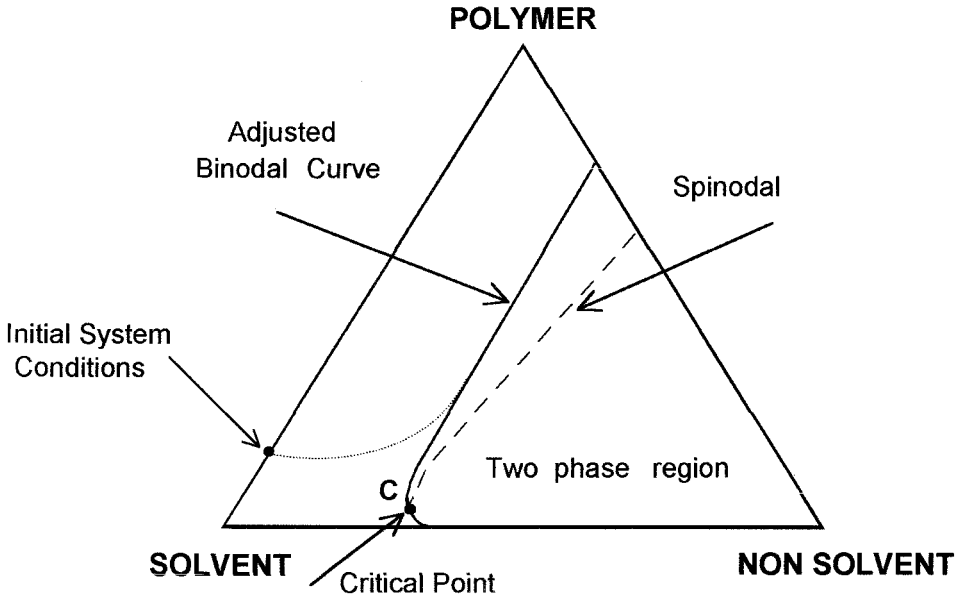

Figure 4 Strategy for the computation of the precipitation time.

Table IV T_s for the AC/Acetone/Water System as a Function of the Precipitation Bath Composition for Two Polymer Concentrations in Casting Solution

Precipitation Bath Composition ϕ (%)		T_s (s)		Experimental Precipitation Time[a] (s)
$\phi_{(1,2)}$	$\phi_{(2,2)}$	$\phi_{(3,1)} = 10\%$	$\phi_{(3,1)} = 15\%$	$\phi_{(3,1)} = 15\%$
0	100	26.7	17.3	19.8
16	84	128	25.1	23.0
36	64	Not detected	46.0	43.0

[a] Reuvers,[1] chapter 6, p 136.

criterion. It is possible to choose other criteria based on spinodal curve, for instance, but this does not seem to be necessary, as shown in the following sections.

RESULTS AND DISCUSSION

The phase-inversion model was used to simulate two different systems that are commonly used for membrane manufacture: AC/acetone/water and PEI/*N*-methylpyrrolidone (NMP)/water. The first system was used to compare the model predictions with published results.[2,3] Simulations were carried out to investigate the effect of solvent addition to the coagulation bath, the effect of nonsolvent addition to the casting solution, and the influence of the initial casting solution thickness (*Lo*) on the polymer concentration profile and casting solution contraction rate. The parameters needed for simulation are presented in Tables I–III, and the partition coefficients were kept equal to 1.0 for solvent and 0.5 for nonsolvent, as discussed before.

Influence of Solvent Concentration in the Coagulation Bath

To investigate the influence of the addition of solvent in the coagulation bath on polymer concentration profiles and casting solution contraction rates, simulations with different initial solvent/nonsolvent concentration ratios were performed for the AC/acetone/water system. The casting solution was assumed to contain 10% polymer and 90% solvent (vol %) in all cases. Different solvent/nonsolvent feed ratios were analyzed for the coagulation bath, including 0/100, 16/84, and 36/64 (vol %). Results are presented in Table IV and in Figures 5 and 6.

Table IV presents the precipitation time calculated through simulation for the AC/acetone/water system and the experimental results obtained by Reuvers.[1] Results are very similar and indicate that the time lag for precipitation increased as solvent was added to the coagulation bath. The simulation results also indicate that the model was able to capture the most important dynamic features of the phase-inversion process.

Figure 5 shows the effect of different solvent/nonsolvent ratios in the coagulation bath on the polymer concentration profiles at precipitation conditions. The addition of solvent to the coagulation bath led to lower interfacial polymer concentration at precipitation conditions and lower polymer concentration gradients at the casting solution. Figure 6 shows how the interface position responded to changes in the coagulation bath composition. The addition of solvent to the coagulation bath delayed the phase-inversion phenomena and led to larger shrinkage of the casting solution.

Qualitatively, the results presented in Figures 5 and 6 agree fairly well with results presented by Tsay and McHugh[3] for other process conditions. According to Tsay and McHugh, the addition of solvent to the coagulation bath causes an increase in thickness and a decrease in density of the membrane skin. These behaviors are confirmed in Figure 5, through simulation. Figures 5 and 6 show very clearly that depending on the initial solvent/nonsolvent concentration ratios in the coagulation bath, membranes with different characteristics can be formed.

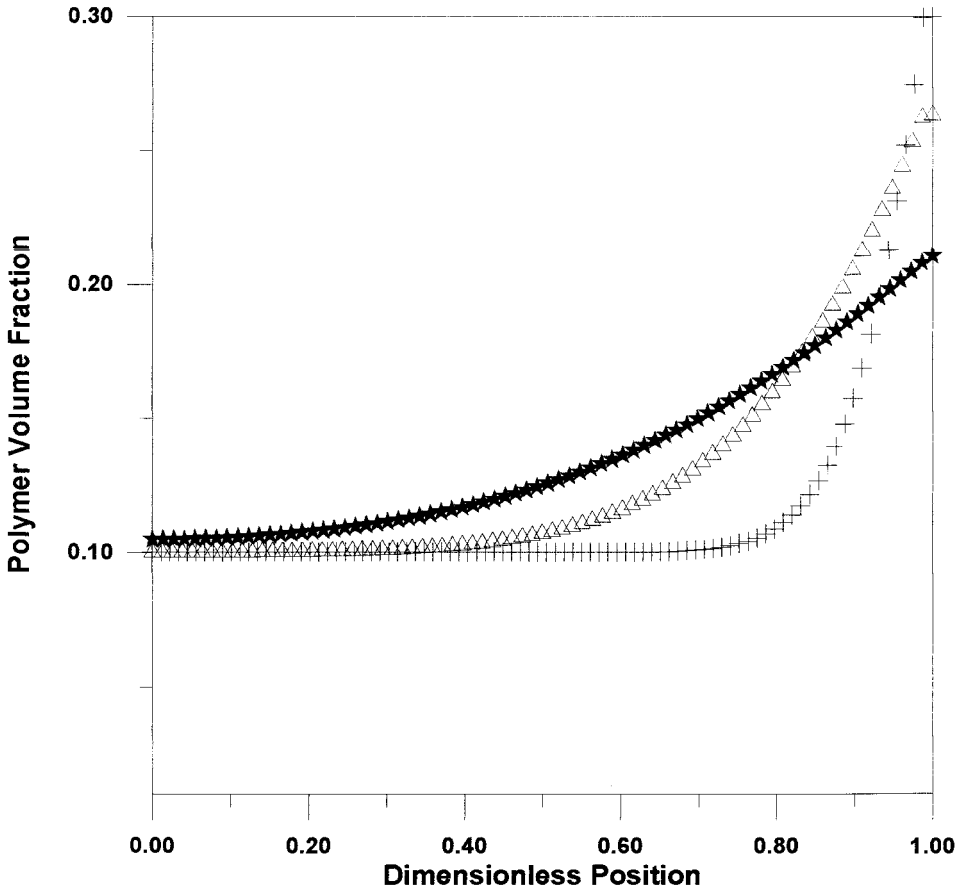

Figure 5 Simulated polymer concentration profiles at precipitation for the AC/acetone/water system for different solvent/nonsolvent coagulation bath compositions. *Lo* = 200 μm. (+) 0/100, simulated precipitation time (T_s) = 26.7 s; (△) 16/84, T_s = 128 s; and (★) 36/64, no precipitation detected. Polymer casting solution: AC/acetone (10/90).

Additional simulation studies were carried out for the PEI/NMP/water system. To our knowledge, no modeling results are available for this system, although experimental data with regard to the membrane formation process can be found in the literature.[2,19] The polymer concentration in the casting solution was assumed to be equal to 10% (vol %), and the casting solution was assumed to contain only polymer and solvent in all simulations. Table V shows the time lag for precipitation for different coagulation bath compositions as obtained through simulation. Figures 7 and 8 show the polymer concentration profiles at the moment of precipitation and the contraction rates of the casting solution as a function of time respectively.

Figure 7 shows that the concentration gradients were very steep in all cases analyzed and that the addition of solvent to the coagulation bath tended to produce less dense membranes as the polymer concentration at the interface decreased. The simulation results (instantaneous precipitation) suggest that very asymmetric membranes were produced in this case, which could be confirmed experimentally.[20] The qualitative behavior of the phase-inversion process for the PEI/NMP/water system resembled very closely the behavior of the AC/acetone/water system, although the first presented much faster precipitation dynamics. For this reason, all interesting dynamics were observed in the spatial region that was located very close to the interfacial boundary.

Figure 8 shows that the total contraction of the casting solution was very small for the PEI/NMP/water system due to the early polymer precipitation, which contributed to the high asymmetry and sublayer porosity of these membranes. The results obtained for the precipitation time, shown in Table V, indicate that precipitation may be

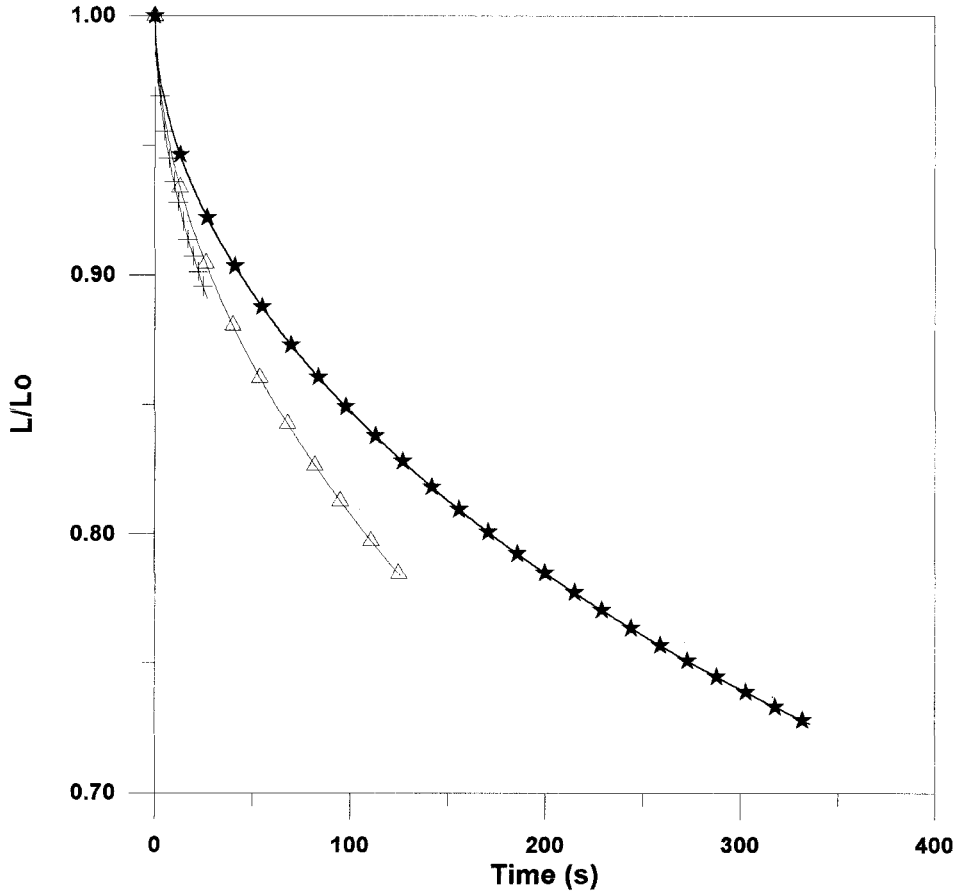

Figure 6 Simulated interface position for the AC/acetone/water system for different solvent/nonsolvent coagulation bath compositions. Lo = 200 μm. (+) 0/100, T_s = 26.7 s; (△) 16/84, T_s = 128 s; and (★) 36/64, no precipitation detected. Polymer casting solution: AC/acetone (10/90).

regarded as instantaneous in this case, confirming experimental results.[19,20] This occurred because the ternary phase diagram of PEI/NMP/water presented a very narrow solubility range, as shown in Figure 3, so that initial feed conditions were always very close to the binodal curve.

Table V T_s for the PEI/NMP/Water System as a Function of the Precipitation Bath Composition

Precipitation Bath Composition ϕ (%)		
$\phi_{(1,2)}$	$\phi_{(2,2)}$	T_s (s)
0	100	0.7
16	84	0.9
36	64	1.5

Polymer casting solution: PEI/NMP = 10/90.

When Figures 5 and 7 and Figures 6 and 8 are compared, one can see that the AC and PEI membranes produced in the conditions analyzed are expected to present different morphologies. AC membranes are expected to be denser and to present much more heterogeneous sublayers, which can be confirmed experimentally.[19,20]

Influence of the Thickness of the Initial Casting Solution

If x is divided by L and t is multiplied by D/L^2 in eqs. (1–14), the model becomes dimensionless. In this case, model solutions obtained are shown to be similar when the boundary conditions are similar in the scaled variables x and t, as shown by Barton et al.[21] (It is assumed in this case that the dimensions of the coagulation bath can be scaled in a similar manner; otherwise, solutions will not

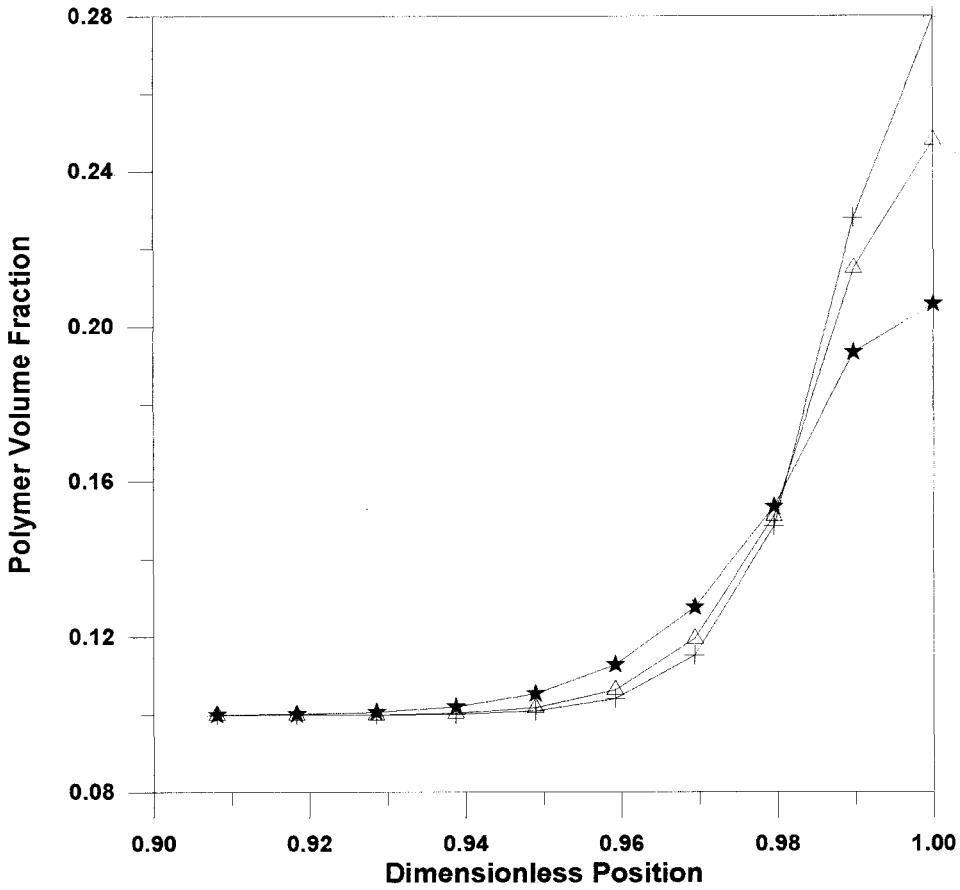

Figure 7 Simulated polymer concentration profiles at precipitation for the PEI/NMP/water system for different solvent/nonsolvent coagulation bath compositions. Lo = 200 μm. (+) 0/100, T_s = 0.7 s; (△) 16/84, T_s = 0.9 s; and (★) 36/64, T_s = 1.5 s.

be equivalent.) This does not mean that resulting membrane characteristics would be the same for three main reasons. First, membrane performance will depend on the absolute values of the skin dimensions and properties. For instance, when similar scaled membranes of different thickness are used at actual separation processes, permeability and selectivity are not necessarily the same. Permeability is expected to decrease, and selectivity, probably, is expected to increase as the membrane thickness increases. Second, during actual membrane preparation, it is not possible to monitor and control the position x of the polymer precipitation front so that similar membranes may be obtained. Actually, membrane preparation is usually carried out in machines where the extrusion velocity (and so, the coagulation time) is kept between well-defined values. Therefore, time and spatial scaling are not preserved in actual preparation conditions. The usual procedure controls the coagulation time, and the excess of the casting solution is discarded (and possibly recovered and recycled). For this reason, the comparison of profiles at similar times may be useful and appropriate. Third, after the formation of the first film of precipitated polymer, the model becomes invalid, as the polymeric phase splits into two different polymer phases. For scaling to be preserved, model formulation for this three-phase system must be equivalent to the model formulation used in the case of two-phase system, which must not be taken for granted given the complex nature of the additional polymer phase. This was also acknowledged by Barton et al.[21] To the best of our knowledge, attempts to model the three-phase system have not yet been made.

To investigate the influence of Lo on polymer concentration profiles and casting solution contraction rates, simulations with different Lo's were performed for the AC/acetone/water system. Typical values used for membrane prepa-

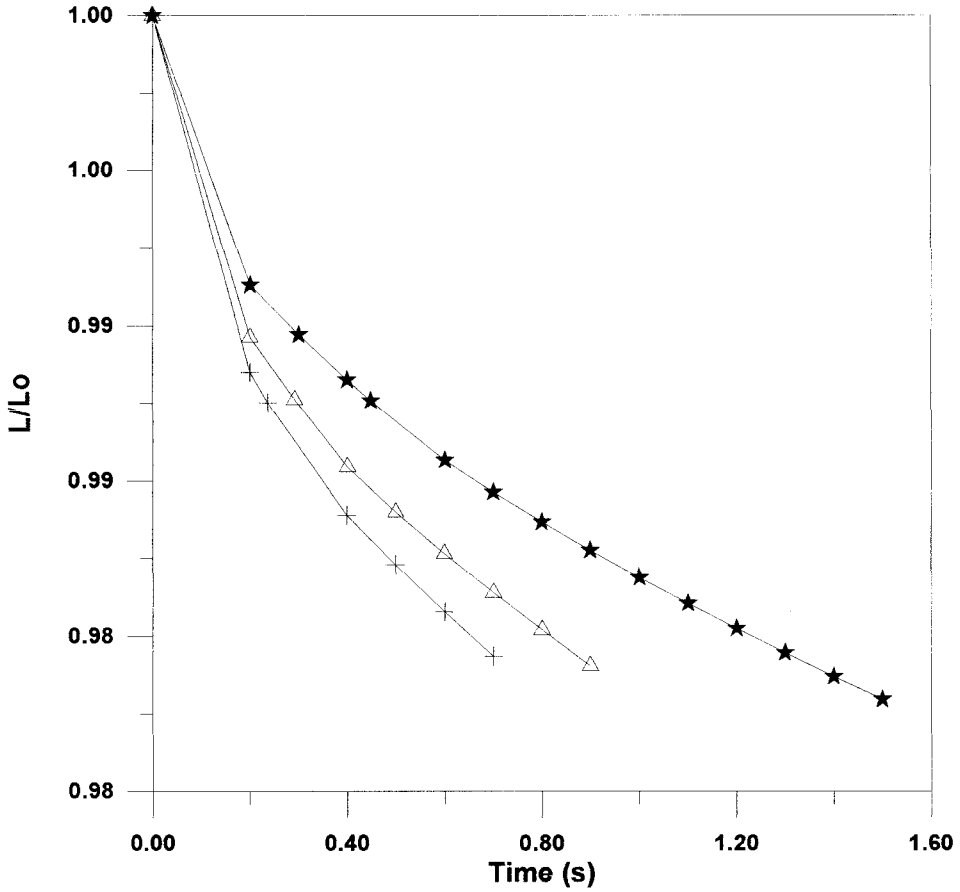

Figure 8 Simulated interface position for the PEI/NMP/water system as a function of the quenching time for different solvent/nonsolvent coagulation bath compositions. *Lo* = 200 μm. (+) 0/100, T_s = 0.7 s; (△) 16/84, T_s = 0.9 s; and (★) 36/64, T_s = 1.5 s.

rations were assumed as 200, 500, and 1000 μm. The casting solution contained 10% polymer and 90% solvent (vol %), whereas the coagulation bath was formed by pure water. As discussed in the previous paragraph, to allow a direct comparison of the results, concentration profiles are presented for similar contact times. It was assumed here that the coagulation bath was much thicker than the casting solution (at least 50 times thicker); otherwise, the amounts of solvent removed from the casting solution would exert a great influence on the precipitation conditions, as shown before. Results are presented in Figures 9–11.

Figure 9 shows polymer concentration profiles after a contact time of 15 s. Polymer concentration gradients were much larger (in dimensionless scale) for thicker casting solutions because a considerable amount of the initial feed behaved as a reservoir of solvent. However, when the absolute scale was analyzed in terms of the distance from the interface, gradients were larger for the thinner casting solutions. This means that thinner skins and more uniform sublayers may be produced when the initial casting solution is thinner. Figure 10 shows that the precipitation dynamics were also much slower when the casting solution was thicker due to the same reasons presented before.

Figure 11 shows the dynamic evolution of the polymer concentration at the interface in the conditions analyzed. Due to the larger amounts of solvent available for mass exchange, the thicker casting solutions led to lower polymer concentrations at equilibrium conditions. This means that denser skins may be produced when the casting film is thin. Interfacial equilibrium was reached after about 0.3–0.5 s in all cases. In all of the simulations studied, it took approximately 0.3–1.0 s for equilibrium to be attained. Therefore, thermodynamic equilibrium between the bulk coagulation bath and the interface was not attained

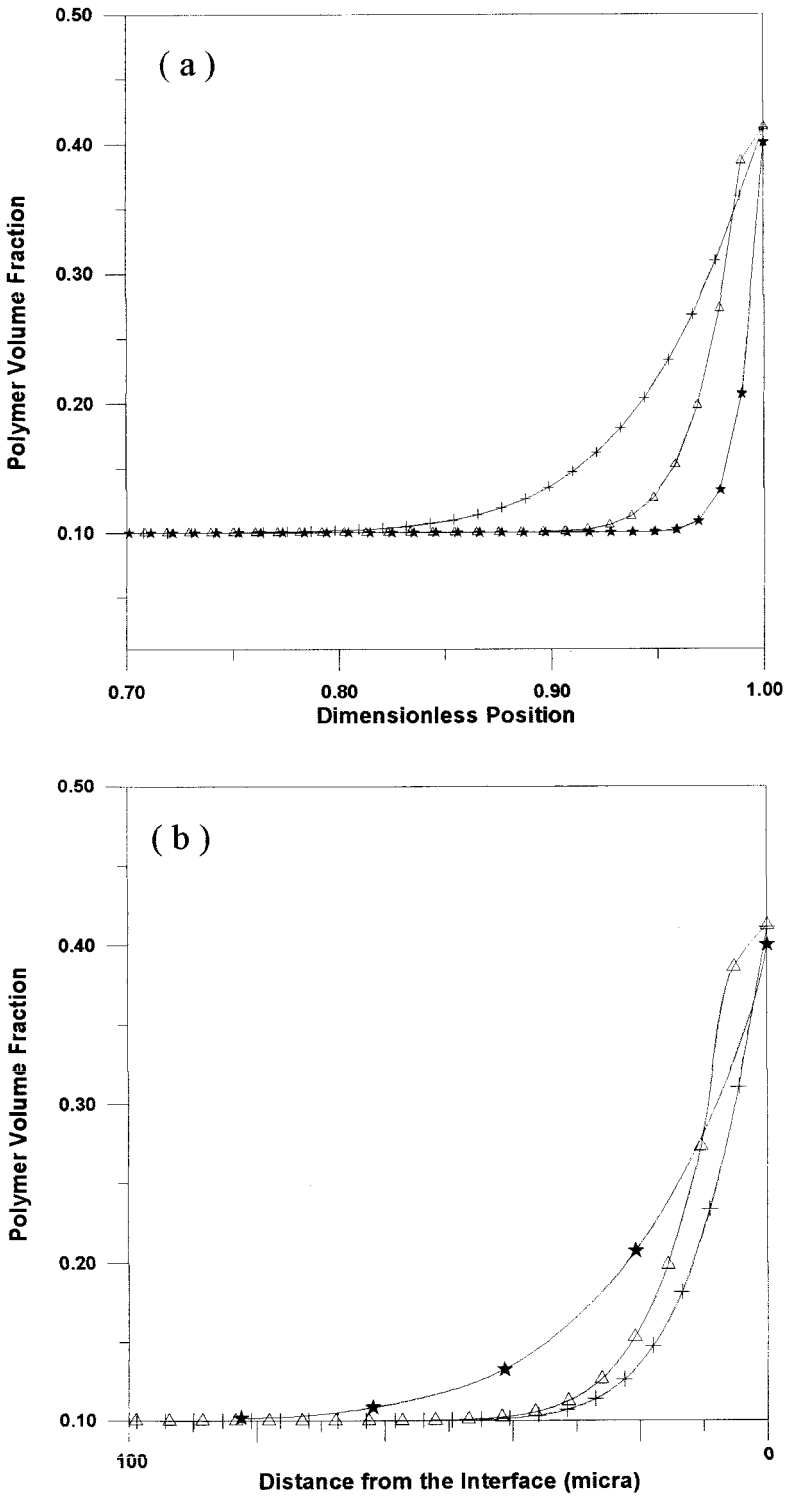

Figure 9 Simulated polymer concentration profiles for the AC/acetone/water system for different *Lo*'s at $t = 15$ s: (+) $Lo = 200$ μm, (△) $Lo = 500$ μm, and (★) $Lo = 1000$ μm. (a) Dimensionless position and (b) distance from interface.

instantaneously, as assumed by Reuvers et al.,[13] and the mass transfer resistance may have played an important role during the very beginning of the phase-inversion process. As the time lag to attain more stable mass transfer conditions may be of the order of magnitude of the precipi-

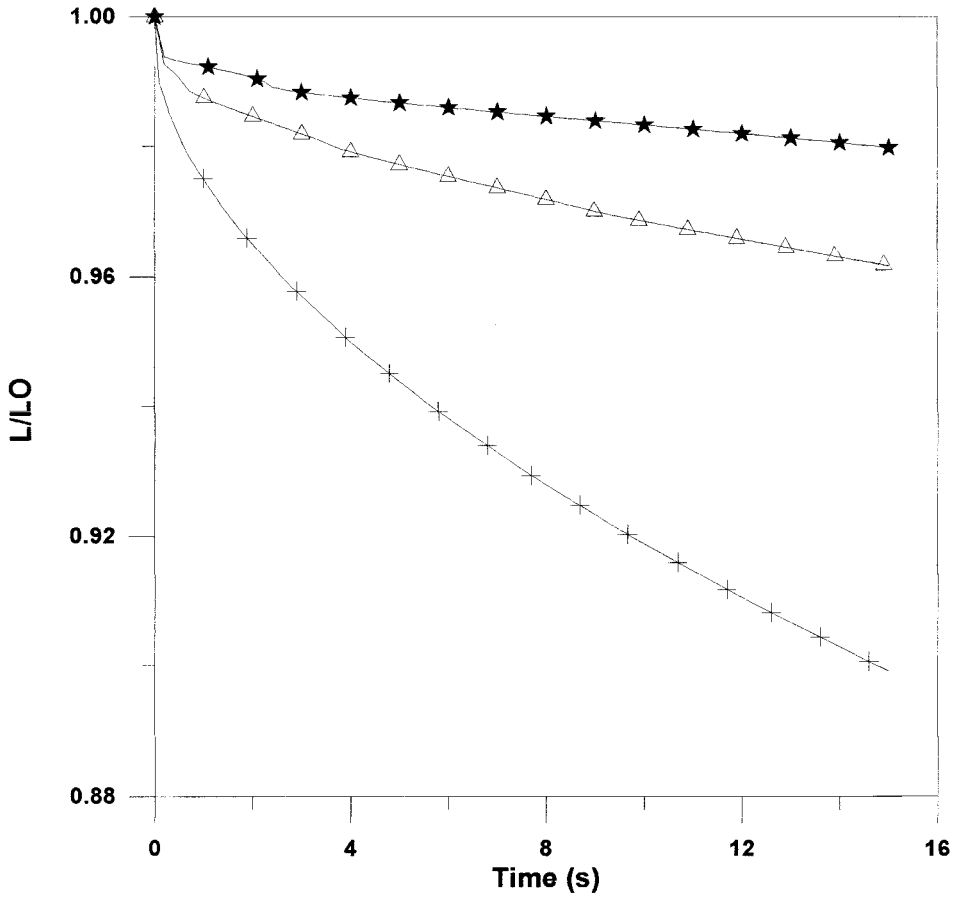

Figure 10 Simulated interface position for the AC/acetone/water system as a function of the quenching time for different *Lo*'s at $t = 15$ s: (+) $Lo = 200$ μm, (△) $Lo = 500$ μm, and (★) $Lo = 1000$ μm.

tation time, precipitation may occur very far from equilibrium for more incompatible systems.

Addition of Nonsolvent to the Casting Solutions

To investigate the influence of the addition of nonsolvent to the initial casting solution on the polymer concentration profiles and casting solution contraction rates, simulations with different initial casting solution concentrations were performed for the AC/acetone/water system. The initial polymer concentration was set to 10% (vol %), and different polymer/solvent/nonsolvent feed ratios were analyzed. The coagulation bath was assumed to contain pure water. Results are presented in Table VI and Figure 12.

Table VI shows that the precipitation time decreased with the increase of water concentration in the polymer casting solution. This expected behavior was related to the fact that with increasing water concentration, the initial polymer casting solution composition came close to the binodal curve. Table VI also presents the experimental precipitation time obtained by Reuvers and Smolders[2] for the AC/acetone/water system. The results are similar and indicate that the time lag for precipitation decreases as water is added to the casting polymer solution. Once more, the simulation results also indicate that the model was able to capture the most important dynamic features of the phase-inversion process.

Figure 12 shows that the increase of the nonsolvent concentration of the casting solution led to an increase in the polymer concentration at the interface and to an increase in the concentration gradients inside the casting solution during precipitation. Both conditions favor the formation of denser and thinner membranes. Besides, the precipitation time was reduced very significantly when small amounts of non-

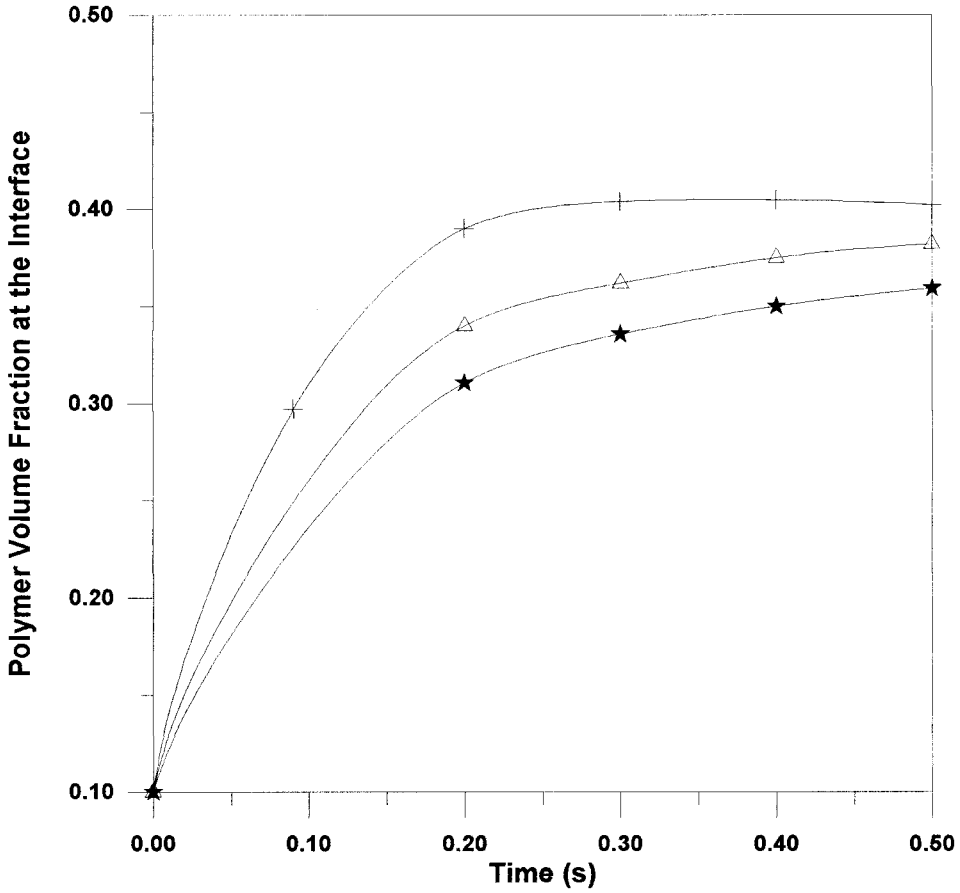

Figure 11 Simulated interface polymer concentration as a function of the quenching time for the AC/acetone/water system for different *Lo*'s: (+) $Lo = 200$ μm, (△) $Lo = 500$ μm, and (★) $Lo = 1000$ μm.

solvent were added to the casting solution. All these results agree very well with the experimental data presented by Tsay and McHugh[3] with regard to the phase inversion of AC/acetone/water systems.

CONCLUSIONS

A simple mass transfer model was developed and implemented to simulate the phase-inversion process, which takes place during mem-

Table VI T_s for the AC/Acetone/Water System as a Function of the Water Content

Polymer Casting Solution Composition ϕ (%)			
$\phi_{(3,1)}/\phi_{(1,1)}/\phi_{(2,1)}$ (AC/Acetone/Water)	Free Polymer Base (Acetone/Water)	T_s (s)	Experimental Precipitation Time[a] (s)
10/90/0	100/00	26.7	26
10/81/9	90/10	12.1	18
10/80/10	88.75/11.25	7.1	—
10/78.75/11.25	87.5/12.5	4.1	0.0
10/76.5/13.5	85/15	0.9	0.0

Precipitation bath: water.
[a] Reuvers and Smolders.[2]

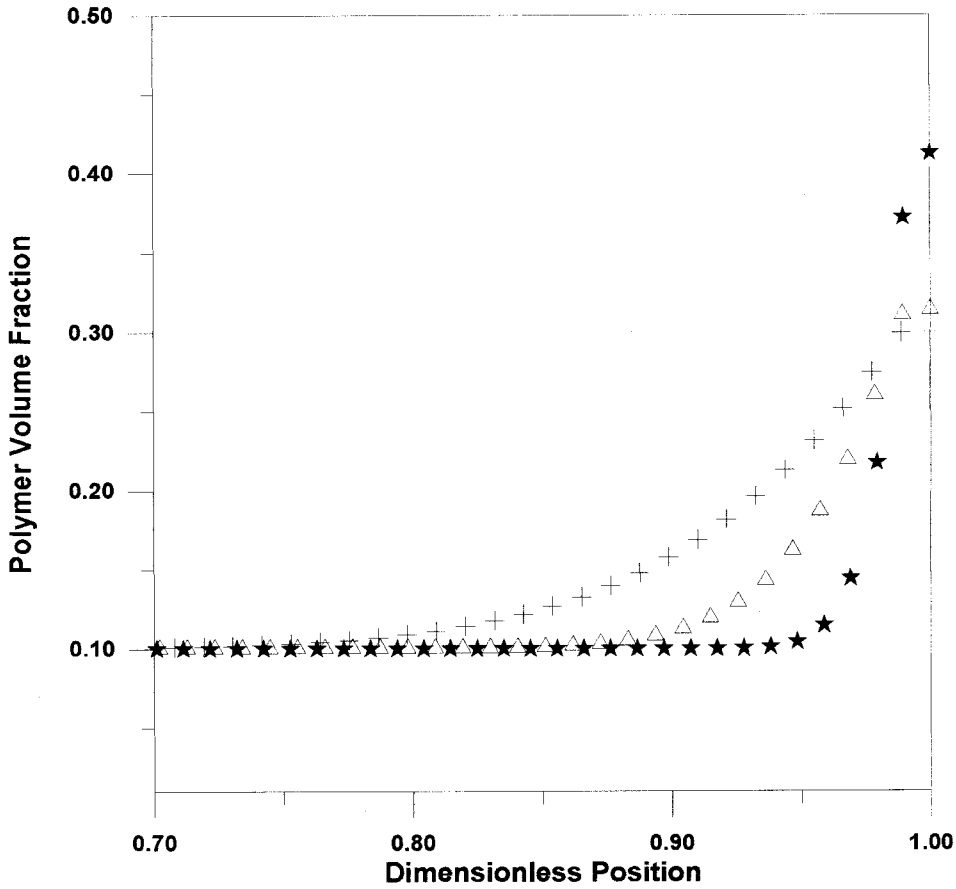

Figure 12 Simulated polymer concentration profiles at precipitation for the AC/acetone/water system for different solvent/nonsolvent casting solution compositions. *Lo* = 200 μm. (+) 10/90/00, T_s = 26.7 s; (△) 10/80/10, T_s = 7.1 s; and (★) 10/76.5/13.5, T_s = 0.9 s. Precipitation bath: water.

brane formation. The model depends on a small number of physical parameters, which are generally available or may be estimated from the literature. The model is able to reproduce both quantitatively and qualitatively experimental results available in published material regarding the morphological aspects of the membranes prepared and the precipitation conditions of the polymer material for the AC/acetone/water and PEI/NMP/water systems. Simulations indicate that (1) the addition of solvent to the coagulation bath leads to less dense and thicker skin layers in the polymeric solution before precipitation and longer time lags for precipitation, (2) the addition of nonsolvent to the casting solution causes the opposite effects, and (3) the reduction of the thickness of the initial casting solutions may cause densification of the skin and the formation of denser membranes. For incompatible systems such as PEI/NMP/water, the precipitation lag may be of the order of magnitude of the time needed for the system to attain a dynamic equilibrium condition, so the assumption of instantaneous equilibrium between the interface and the bulk solution may lead to large model deviations in these cases. Finally, it was shown for both polymeric systems investigated in this work that the dynamics of the mass transfer process seem to be much more important than the influence of the concentration on the diffusion and thermodynamic partition coefficients, as fair agreement with available experimental data was obtained even when these coefficients were assumed to be constant.

The authors thank Conselho Nacional de Desenvolvimento Científico e Tecnológico for scholarships and support of this research.

NOMENCLATURE

Abbreviations

AC	cellulose acetate
NC	number of chemical species
NMP	*N*-methylpyrrolidone
PEI	polyetherimide

Symbols

A	mass transfer area (m^2)
$C_{(i,j)}$	molar concentration of component i in phase j (kg/m^3)
$C^*_{(i,j)}$	mass concentration of component i in phase j (mol/m^3)
$D_{(i,j)}$	diffusion coefficient of component i in phase j (m^2/s)
$k_{(i)}$	partition coefficient of component i (dimensionless)
L	casting solution thickness at time t (m)
Lo	initial casting solution thickness (m)
$M_{(3,1)}$	total polymer mass in polymer solution (kg)
$Pm_{(i)}$	molecular weight of component i (kg/kmol)
T_s	simulated precipitation time (s)
x	mass transfer direction (m)
$x(0)$	initial interface position (m)—Figure 1
$x(t)$	interface position at time t (m)—Figure 1

Greek

$\phi_{(i,j)}$	volume fraction of component i in phase j (dimensionless)
$\rho_{(i,j)}$	density of component i in phase j (kg/m^3)
$\rho_{(i)}$	density of pure component i (Kg/m^3)

Index (*i,j*)

First Index (i)

1. Solvent
2. Nonsolvent
3. Polymer

Second Index (j)

1. Polymer solution phase
2. Precipitation bath phase

REFERENCES

1. Reuvers, A. J. Ph.D. Thesis, Twente University of Technology, Twente, The Netherlands, 1987.
2. Reuvers, A. J.; Smolders, C. A. J Membr Sci 1987, 34, 67.
3. Tsay, C. S.; McHugh, A. J. J Polym Sci Part B: Polym Phys 1990, 28, 1327.
4. Nobel, R. D.; Stern, S. A. Membrane Separations Technology—Principles and Applications; Elsevier Science: Amsterdam, 1995.
5. McHugh, A. J.; Tsay, C. S. J Membr Sci 1991, 64, 81.
6. Castellari, C.; Ottani, S. J Membr Sci 1981, 9, 29.
7. Cheng, L. P.; Soh, Y. S.; Dwan, A. H.; Gryte, C. C. J Polym Sci Part B: Polym Phys 1994, 32, 1413.
8. Cheng, L. P.; Lin, D. J.; Shih, C. H.; Dwan, A. H.; Gryte, C. C. J Polym Sci Part B: Polym Phys 1999, 37, 2079.
9. Termonia, Y. J Membr Sci 1995, 104, 173.
10. Tsay, C. S.; McHugh, A. J. J Polym Sci Part B: Polym Phys 1991, 29, 1261.
11. McHugh, A. J.; Tsay, C. S.; Barton, B. F.; Reeve, J. L. J Polym Sci Part B: Polym Phys 1995, 33, 2179.
12. Radovanovic, P.; Thiel, S. W.; Hwang, S. T. J Membr Sci 1992, 65, 213.
13. Reuvers, A. J.; van den Berg, J. W. A.; Smolders, C. A. J Membr Sci 1987, 34, 45.
14. Shojaie, S. S.; Krantz, W. B.; Greenberg, A. R. J Membr Sci 1994, 94, 255.
15. Brandup, J.; Immergut, E. H. Polymer Handbook, 3rd ed.; Wiley: New York, 1989.
16. Reid, R. C.; Prausnitz, J. M.; Poling, B. E. The Properties of Gases and Liquids, 4th ed.; McGraw-Hill: New York, 1987.
17. Petzold, L. R. DASSL Code, version 1989; Computing and Mathematics Research Division, Lawrence Livermore National Laboratory: Livermore, CA, 1989.
18. Furtado, C. J. A. M.S. Thesis (in Portuguese), PEQ/COPPE/UFRJ, Rio de Janeiro, Brazil, 1993.
19. Wang, D. L.; Li, K.; Teo, W. K. J Appl Polym Sci 1999, 71, 1789.
20. Roesink, E. Ph.D. Dissertation, University of Twente, Twente, Enschede, The Netherlands, 1989.
21. Barton, B. F.; Reeve, J. L.; McHugh, A. J. J Polym Sci Part B: Polym Phys 1997, 35, 569.